Research Article

# Influence of perforation and sound-absorbing material filling on acoustic attenuation performance of three-pass perforated mufflers

Hongpu Huang[1,2] (iD), Zhenlin Ji[1] and Zhuoliang Li[1]

## Abstract

The finite element method is employed to calculate the transmission loss of three-pass perforated reactive and hybrid mufflers. The effects of perforated tubes and bulkheads on the transmission loss of three-pass reactive mufflers are investigated numerically. Two types of hybrid mufflers are considered, and the effects of sound-absorbing material filling and packed outlet tube on the acoustic attenuation performance of mufflers are analyzed. The perforations of the tubes and bulkheads and sound-absorbing material filling are demonstrated to have significant influence on the acoustic attenuation behaviors of the mufflers. The perforation of the tubes and bulkheads may shift the resonance from the low- to middle-frequency range. The sound-absorbing material filling in the middle chamber improves the acoustic attenuation performance at middle to higher frequencies and provides a relatively flat and broadband acoustic attenuation. It is found that the solid inlet or outlet tube replacing the perforated tube and sound-absorbing material filling in the middle chamber increases the pressure drops, while the rest configurations change the pressure drops slightly.

## Keywords

Three-pass perforated muffler, acoustic attenuation performance, finite element analysis, perforation, sound-absorbing material

## Introduction

Three-pass perforated (TPP) muffler is a highly desirable device to reduce the vehicle's exhaust noise with reasonable low backpressure. Dickey et al.[1] developed a one-dimensional (1D) time-domain approach to predict the acoustic attenuation performance of the typical TPP muffler. Munjal[2,3] and Selamet et al.[4] then proposed the corresponding 1D frequency-domain computational approaches to determine the acoustic attenuation performance of the TPP mufflers. The 1D approaches are valid only at low frequencies since these studies assumed the plane wave propagation in the axial direction and excluded the effect of three-dimensional (3D) waves inside the mufflers. The

numerical methods such as finite element method (FEM) and boundary element method (BEM) are no longer confined to a plane wave treatment. Ross[5] introduced the FEM to determine the transmission loss of simple perforated muffler using the measured acoustic impedance of perforation. His predictions showed good

[1]College of Power and Energy Engineering, Harbin Engineering University, Harbin, P.R. China
[2]Guangxi Liugong Machinery Co., Ltd., Liuzhou, P.R. China

**Corresponding author:**
Zhenlin Ji, College of Power and Energy Engineering, Harbin Engineering University, Harbin 150001, Heilongjiang, P.R. China.
Email: jizhenlin@hrbeu.edu.cn

agreement with the measurements at low frequencies. Ji and Selamet[6] applied the substructure BEM to predict the acoustic attenuation performance of TPP mufflers. The effects of length and porosity of perforation, lengths of the expansion chamber and the end cavities, as well as duct extensions into the end cavities on the acoustic attenuation performance of TPP mufflers were investigated in detail. Ji and Fang[7] employed the 1D plane wave theory and 3D FEM to predict the transmission loss of the TPP mufflers with end resonator. Their study showed that the end resonator may improve the acoustic attenuation performance of the TPP muffler at low frequencies. Munjal and Krishna[8] applied transfer matrix method to predict the transmission loss of the three-pass double reversal muffler which consists of three perforated tubes and presented a flow-resistance network approach to evaluate the mean flow distribution. Verma and Munjal[9] investigated the effects of the absorptive material, porosity of the baffle plates, porosity of the perforated tubes, as well as the length of perforation of the perforated tubes on the acoustic attenuation performance of a three-chamber U-bend hybrid muffler by 1D transfer matrix method and 3D FEM.

However, to the knowledge of the authors, the study on the TPP mufflers with perforations on the inlet and outlet tubes within the end cavities and the bulkheads, as well as the sound-absorbing material filling, has not been published, which is widely used in the practical engineering. The objective of this study is then to investigate the effects of the perforations on the tubes and bulkheads as well as the sound-absorbing material filling on the acoustic attenuation performance of TPP mufflers using the 3D FEM. The study may provide the guidelines for TPP muffler designs.

Following the introduction, section "FEM and experimental validation" describes the FEM and experimental validation briefly, section "Results and discussions" exhibits the influence of perforation and sound-absorbing material filling on the acoustic attenuation performance and flow resistance, and section "Conclusion" concludes the study with final remarks.

## FEM and experimental validation

### FEM

The sound pressure inside the muffler is controlled by the Helmholtz equation[10]

$$\nabla^2 p + k^2 p = 0 \tag{1}$$

The equation can be solved numerically by the FEM. With Galerkin's method of weighted residuals, the finite element (FE) equation is expressed as follows

$$([M] - k^2[K])\{p\} = -j\rho_0\omega\{F\} \tag{2}$$

where $[K]$ and $[M]$ are the global stiffness matrix and mass matrix, respectively, $\{F\}$ is the global forcing vector, $p$ is the sound pressure, $k$ is the wavenumber, $\omega$ is the circular frequency, $j$ is the unit imaginary number, and $\rho_0$ is the density of the medium.

For the TPP mufflers in this study, there are four boundary conditions (BCs) as follows:

1. The rigid wall

$$\frac{\partial p}{\partial n} = 0 \tag{3}$$

2. The inlet with normal particle velocity ($v$)

$$\frac{\partial p}{\partial n} = j\omega\rho_0 v \tag{4}$$

3. The outlet with impedance ($Z_p$)

$$\frac{\partial p}{\partial n} = \frac{j\omega\rho_0 p}{Z_p} \tag{5}$$

4. The perforated surface.

The sound pressure difference and the normal particle velocity $v_n$ on perforated section are related as follows

$$\xi_p = \frac{p_1 - p_2}{\rho_0 c_0 v_n} = \frac{R_h + jX_h}{\varphi} \tag{6}$$

$$R_h = \frac{\sqrt{8\rho_0\mu\omega}(1 + t_w/d_h)}{\rho_0 c_0} \tag{7}$$

$$X_h = k(t_w + \alpha d_h) \tag{8}$$

where $\xi_p$ is the specific acoustic impedance of perforation, $\varphi$ is the porosity, $\mu$ is the dynamic viscosity, $t_w$ is the thickness of perforated tube, $d_h$ is the hole diameter, $c_0$ is the speed of sound, and $\alpha$ is the end correction coefficient[11]

$$\alpha = \frac{4}{\pi^2(\zeta\eta)^{0.5}} \sum_{m=0}^{\infty} \sum_{n=0}^{\infty} {}' \varepsilon_{mn} \frac{J_1^2\left(\pi\sqrt{(m\zeta)^2 + (n\eta)^2}\right)}{(m^2(h/b) + n^2(b/h))^{1.5}} \tag{9}$$

where $\zeta = d_h/b$, $\eta = d_h/h$, $b$, and $h$ are the distances between two neighboring holes in two directions; the prime on the summation sign implies that the term representing the (0, 0) fundamental mode is excluded;
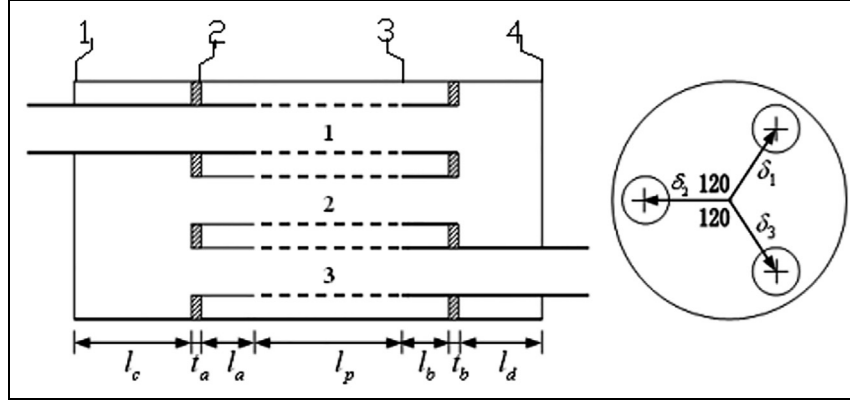
**Figure 1.** Three-pass perforated tube muffler with circular cross section.

$\varepsilon_{mn} = 1$ if $m \neq 0$, $n \neq 0$ and $\varepsilon_{mn} = 1/2$ if otherwise; and $J_1$ is the Bessel function of the first kind of order 1.

When one side of the perforation is attached by the sound-absorbing material, the acoustic impedance of perforation is modified as follows[12]

$$\xi_p = \frac{R_h + jk\left(t_w + 0.5\alpha\left(1 + (\tilde{k}/k)(\tilde{z}/z)\right)d_h\right)}{\varphi} \quad (10)$$

The sound-absorbing material can be described as the equivalent fluid with complex impedance $\tilde{z}$ and complex wavenumber $\tilde{k}$,[13,14] which may be expressed as follows

$$\frac{\tilde{z}}{z} = \left(1 + a_1 f^{-b_1}\right) - ja_2 f^{-b_2} \quad (11)$$

$$\frac{\tilde{k}}{k} = \left(1 + a_3 f^{-b_3}\right) - ja_4 f^{-b_4} \quad (12)$$

In this study, the fiberglass used by Lee and Selamet[14] is selected as the absorbing material. The average diameter of the fibers $d_f = 24\,\mu$m. For this fiberglass with the bulk density of 100 g/L, the porosity is 96.7%, the flow resistivity $R_f = 4,896$ Rayls/m, $a_1 = 33.2$, $b_1 = 0.7523$, $a_2 = 28.32$, $b_2 = 0.6512$, $a_3 = 39.2$, $b_3 = 0.6841$, $a_4 = 38.39$, $b_4 = 0.6285$, while for the same material with the bulk density of 200 g/L, the porosity is 93.3%, the flow resistivity $R_f = 17,378$ Rayls/m, $a_1 = 25.69$, $b_1 = 0.5523$, $a_2 = 71.97$, $b_2 = 0.7072$, $a_3 = 56.03$, $b_3 = 0.6304$, $a_4 = 62.05$, $b_4 = 0.5980$.

### Transmission loss

The transmission loss is used to evaluate the acoustic attenuation performance of TPP mufflers. It can be calculated by the following equation in the frequency range below the plane wave cut-off frequencies of the inlet and outlet tubes

$$TL = 20 \log 10\left[(S_1/S_2)^{1/2}|p_i/p_t|\right] \quad (13)$$

where $S_1$ and $S_2$ are the cross-sectional areas of the inlet and outlet tubes, respectively, $p_i$ is the incident sound pressure in the inlet tube, and $p_t$ is the transmitted sound pressure in the outlet tube.

### Validation

The FEM software COMSOL Multiphysics is employed to calculate the transmission loss of mufflers. The measurement of transmission loss may be found in the work by Tao and Seybert.[15]

In order to verify the accuracy of FEM, the typical TPP muffler shown in Figure 1 is chosen to compare the transmission loss predictions with measurements. The muffler has the inner diameter of $D = 165.1$ mm. The three perforated tubes have the inner diameter of $d = 48.9$ mm, the tube thickness of $t_w = 0.8$ mm, the perforated diameter of $d_h = 2.34$ mm, and perforated porosity of $\varphi = 4.5\%$. The tube offset distances from the center of the muffler are $\delta_1 = \delta_2 = \delta_3 = 39.7$ mm. The bulkhead thickness is $t_a = t_b = 12.7$ mm. The rest of the dimensions are $l_a = l_b = 27.9$ mm, $l_c = 150$ mm, $l_d = 102$ mm, $l_p = 274$ mm. The speed of sound is $c_0 = 344$ m/s and the density of air is $\rho_0 = 1.225$ kg/m³.

The muffler shell is set as the transparent vision to view the internal structure of the muffler shown in Figure 2. The blue and red regions represent the perforated and solid tubes, respectively. The hexahedral element is used with a maximum element size of 15 mm, which ensures the accuracy of predictions in the frequency range of interest.[16] Figure 3 exhibits that the FEM prediction of the transmission loss agrees well with the measurements.[6] It may be seen that the 1D analytic results match the measurements well only up to the plane wave cut-off frequency due to the exclusions of higher order modes.
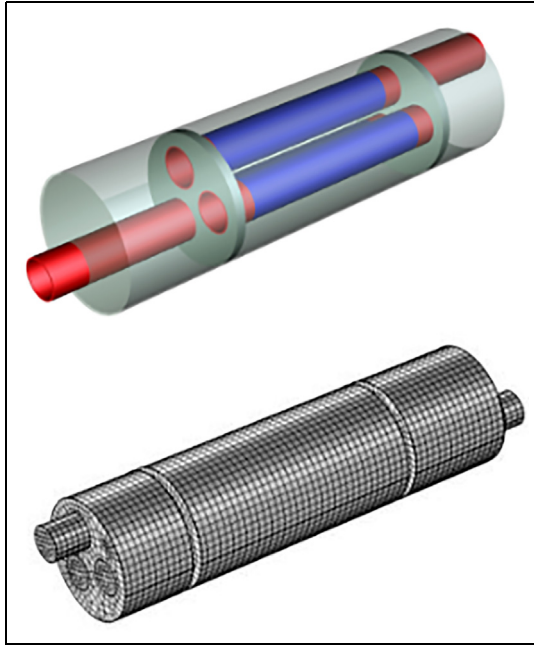
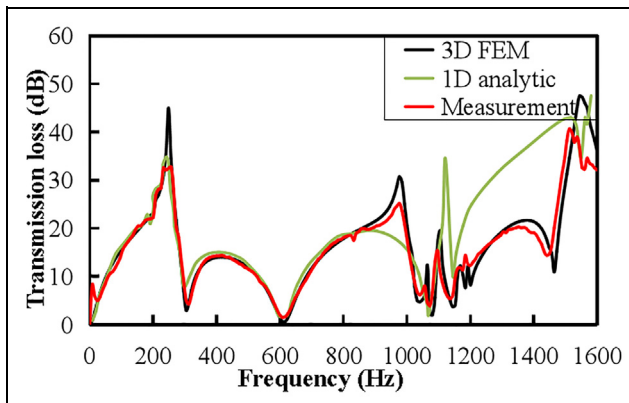**Figure 2.** Geometry and FE mesh of three-pass perforated muffler with circular cross section.



**Figure 3.** Transmission loss of three-pass perforated muffler with circular cross section.
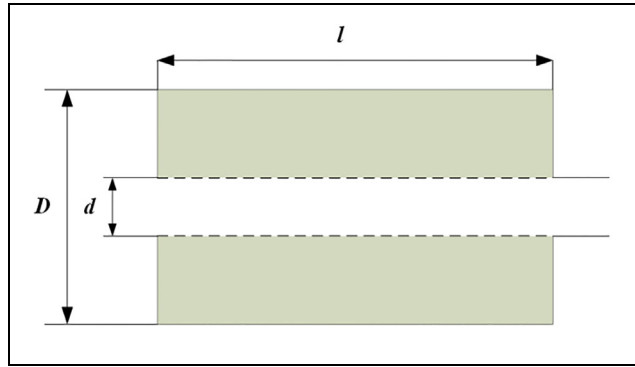


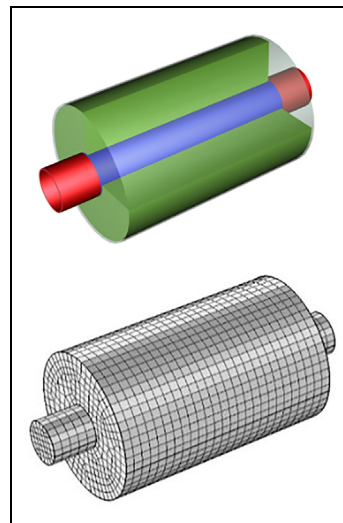**Figure 4.** Straight-through perforated tube dissipative muffler.



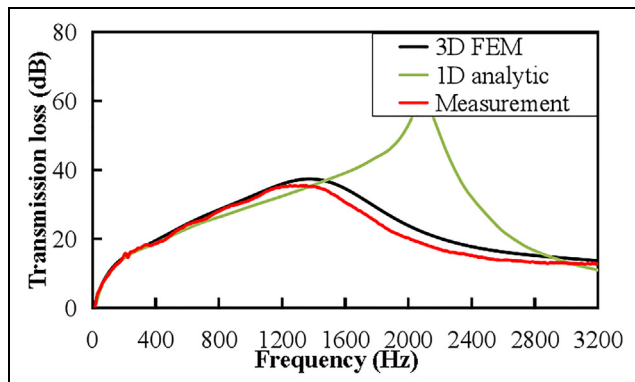**Figure 5.** Geometry and FE mesh of straight-through perforated dissipative muffler.
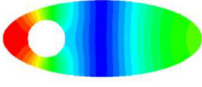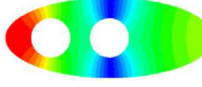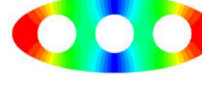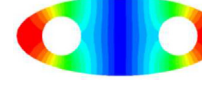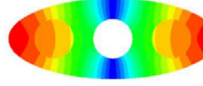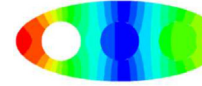


**Figure 6.** Transmission loss of straight-through perforated dissipative muffler.

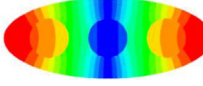Figure 4 shows the straight-through perforated tube dissipative muffler. The chamber has the inner diameter of $D = 164.4$ mm and the length of $l = 257.2$ mm. The perforated tube has the inner diameter of $d = 49$ mm, the tube thickness of $t_w = 0.9$ mm, the perforated diameter of $d_h = 4.98$ mm, and perforated porosity of $\varphi = 8.4\%$.

The 3D geometrical model and FE mesh of the muffler are shown in Figure 5. The green color denotes the sound-absorbing material. Figure 6 compares the transmission loss predictions and measurements of the straight-through perforated tube dissipative muffler. The FEM predictions coincide reasonably well with the measurements, while the discrepancy at high-frequency range may possibly be attributed to (1) the assumption of the isotropic sound-absorbing material and (2) the approximated acoustic impedance of perforation. The

**Table 1.** The plane wave cut-off frequencies on the cross sections of the configurations in Figure 7.

| Mode | Section A | Section B | Section C | Section E |
|---|---|---|---|---|
| First order |  |  |  |  |
| | 780.0 Hz | 686.9 Hz | 698.8 Hz | 774.5 Hz |

| Mode | Section D Baseline | Section D Solid center tube | Section D Solid inlet/outlet tube |
|---|---|---|---|
| First order |  |  |  |
| | 683.7 Hz | 636.3 Hz | 713.9 Hz |
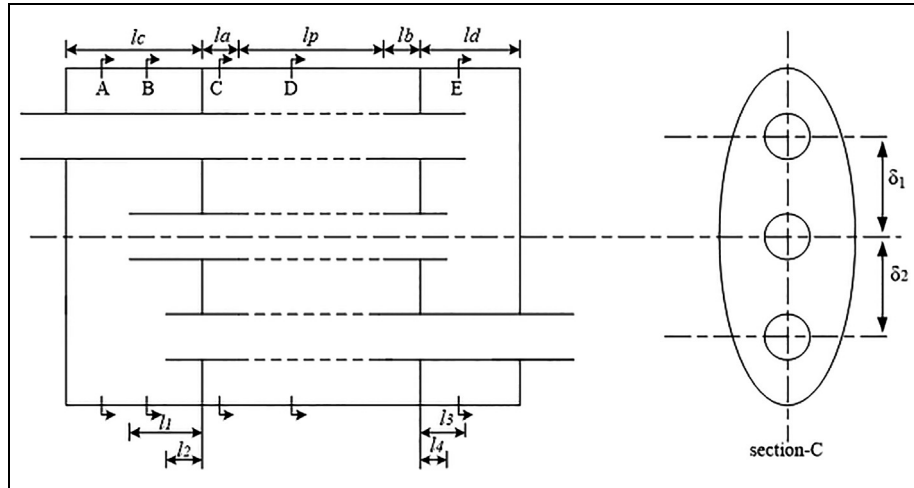


**Figure 7.** Three-pass reactive muffler (baseline configuration).

results show the agreement between 1D analytic results and measurements in the lower frequency range.

## Results and discussions

Considering the limited design space in the practical application, the TPP muffler with elliptical cross section is the commonly used configuration shown in Figure 7. In this section, the effects of the number of perforated tubes within the middle chamber, the perforation of the tubes within the end cavities, as well as perforated bulkheads on the transmission loss are investigated numerically. Two types of hybrid mufflers are considered then, and the effects of sound-absorbing material filling and packed outlet tube on the acoustic attenuation performance of TPP mufflers are analyzed. In the last subsection, the pressure drops of different configurations are predicted using the software ANSYS Fluent.

### Reactive mufflers with perforated tubes

The elliptical cross section of the muffler has the major axis and minor axis of $D = 260$ mm, $d = 100$ mm. The perforated tubes have the inner diameter of $d = 48.8$ mm, the tube thickness of $t_w = 1.5$ mm, the perforated diameter of $d_h = 2.5$ mm, and perforated porosity of $\varphi = 6\%$. The offsets of inlet and outlet tubes are $\delta_1 = \delta_2 = 73$ mm. The rest of the dimensions are $l_1 = 80$ mm, $l_2 = 40$ mm, $l_3 = 50$ mm, $l_4 = 30$ mm, $l_a = l_b = 40$ mm, $l_c = 150$ mm, $l_d = 107$ mm, $l_p = 160$ mm.

In order to indicate the necessity of using the 3D method for the acoustic attenuation analysis in the frequency range of interest, the plane wave cut-off frequencies of the various cross sections shown in Figure 7 are determined first using the 2D FEM.[17] The plane wave cut-off frequency corresponds to the first-order
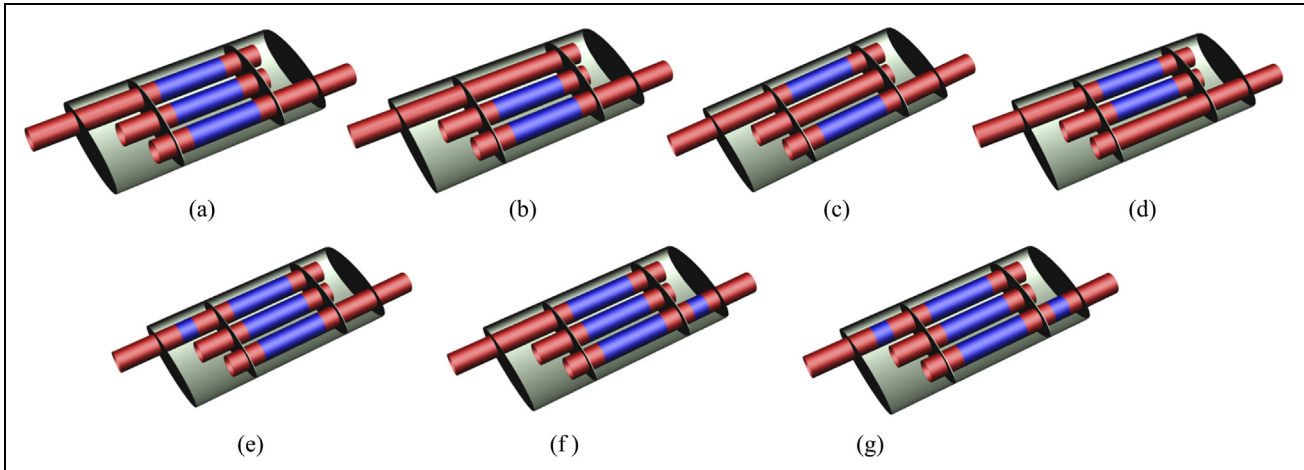
**Figure 8.** Configurations of three-pass reactive mufflers: (a) baseline, (b) solid inlet tube, (c) solid center tube, (d) solid outlet tube, (e) perforation on inlet tube within the inlet chamber, (f) perforation on outlet tube within the outlet chamber, and (g) perforations on inlet and outlet tubes within the inlet and outlet chambers (blue region: perforated portion; red region: solid portion).
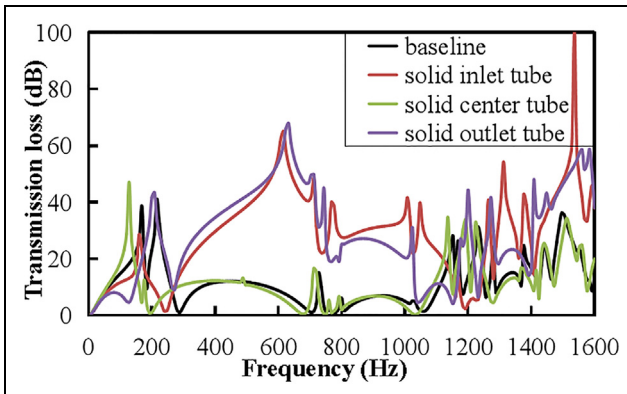


**Figure 9.** Effect of perforated tubes on transmission loss of three-pass reactive muffler.

modal frequency as the perforated tubes are not located on the nodal line of the first-order mode. Table 1 demonstrates that the effect of different cross-sectional configurations on the plane wave cut-off frequencies is noticeable.

All configurations of three-pass reactive mufflers with perforated tubes considered in this subsection are shown in Figure 8.

The effect of perforated tubes within the middle chamber on the transmission loss is examined with keeping other parameters unchanged. Figure 9 shows the transmission loss predictions of the mufflers with different perforated tubes. The baseline configuration may be decomposed into three acoustic elements (one expansion chamber and two end cavities). The first two resonance peaks of the transmission loss are attributed to the two end cavities with the two inserted tubes. The end cavity works as the chamber of Helmholtz resonator, while the two inserted tubes form an equivalent

neck. The resonance frequency of the resonator is directly proportional to the square root of the cross-sectional area of the neck and inversely proportional to the square root of the length of the neck and the volume of the chamber. When removing the perforation of the inlet tube, the right end cavity and the middle chamber form a double-expansion chamber, while the left end cavity still works as a resonator. This change leads to the disappearance of the second resonance peak. The double-expansion chamber creates huge discrepancy beyond the resonance frequency compared to the baseline muffler and enhances the acoustic attenuation in the mid-frequency range (300–1200 Hz). Similar behavior is held for the muffler with solid outlet tube. When the perforated center tube is replaced by the solid tube, the two end cavities form a dual-chamber resonator which exhibits a lower frequency resonance than the baseline. The middle chamber keeps the same role working as an expansion chamber, so the acoustic attenuation performance changes slightly in the middle-to high-frequency range.

The effect of perforation on the inlet and outlet tubes within the end cavities on the acoustic attenuation performance of the muffler is examined next. In this study, one row of holes with diameter $d_h = 5$ mm is located at the center position. Figure 10 shows that increasing the number of holes on the inlet tube shifts the first resonance peak to higher frequency, while the second resonance peak remains unchanging. The holes on the inlet tube within the left end cavity and the two solid portions of the center and outlet tubes work together as the neck of left end resonator; therefore, the enlarged equivalent area of the neck of the resonator shifts the resonance to higher frequency. Similarly, the perforation of the outlet tube shifts the second
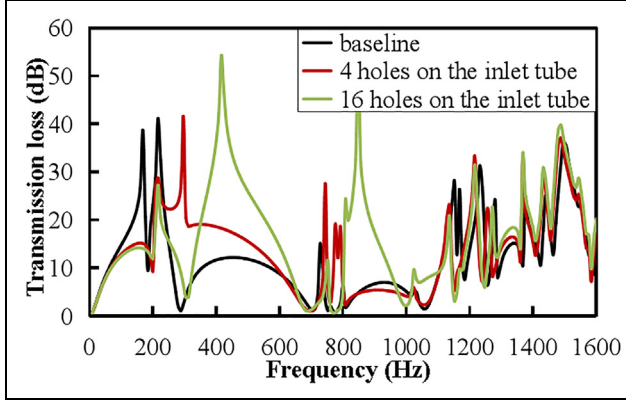
**Figure 10.** Effect of inlet tube perforation on transmission loss of three-pass reactive muffler.
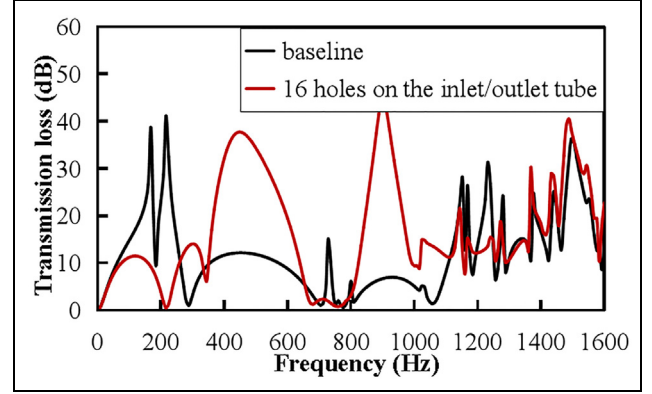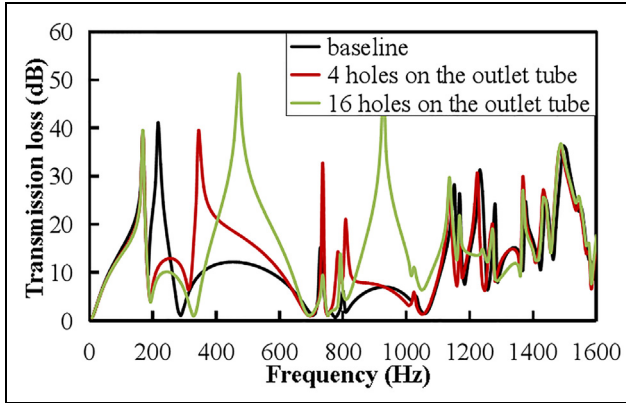


**Figure 11.** Effect of outlet tube perforation on transmission loss of three-pass reactive muffler.

resonance peak to higher frequency as shown in Figure 11. When the holes are drilled on both the inlet and outlet tubes, the first and the second resonance peaks are shifted to higher frequency. The two peaks are combined together to form a smooth wide resonance (400–600 Hz) as shown in Figure 12. Comparison of the two curves illustrates that the influence of the perforation within the end cavities on the acoustic attenuation performance in high-frequency range is marginal.

### Reactive mufflers with perforated bulkheads

The configurations of three-pass reactive mufflers with perforated bulkheads are shown in Figure 13. The bulkheads are perforated with the hole diameter $d_h = 2.5$ mm.

The effect of perforated bulkheads on the transmission loss of the three-pass reactive muffler is demonstrated in Figure 14. The mufflers with perforated bulkheads reveal the similar acoustic behavior to the



**Figure 12.** Effect of inlet and outlet tube perforations on transmission loss of three-pass reactive muffler.

mufflers with perforations on the inlet or/and outlet tubes within the end cavities in low- to mid-frequency range, which shifts the associated resonance peak to higher frequency. For all configurations with perforated bulkheads, a wider attenuation band in low-frequency range is observed, while the influence on the acoustic attenuation in high-frequency range is complex somewhat.

The effect of porosity of the inlet bulkhead on the transmission loss of the muffler is illustrated in Figure 15. It may be seen that increasing the porosity shifts the second resonance peak to higher frequency, while the influence on acoustic attenuation in high-frequency range is not remarkable.

### Hybrid muffler with perforated tubes

Figure 16 depicts the transmission loss predictions of the mufflers with sound-absorbing material filling in the middle chamber, which provides a flat broadband transmission loss. The higher bulk density of sound-absorbing material leads to the higher acoustic attenuation at middle to higher frequencies.

### Hybrid muffler with packed outlet tube

Assembling the outlet tube with a sleeve tube packed and the sound-absorbing material filled inside forms a kind of hybrid muffler as shown in Figure 17, which may provide better acoustic performance in wider frequency range. This study considers $l_m = 60$ mm, $l_n = 20$ mm, $d_2 = 70$ mm for the inner diameters of the sleeve tube, $d_h = 2.5$ mm, for the hole diameter of the inner perforated tube, $\varphi = 20\%$, for the porosity of the inner perforated tube. Different number (perforation) of holes (diameter 2.5 mm) on the "$l_m$" part and different bulk densities of the sound-absorbing material will be discussed.

The 3D geometrical model used in the acoustic analysis of the mufflers with packed outlet tube is shown in
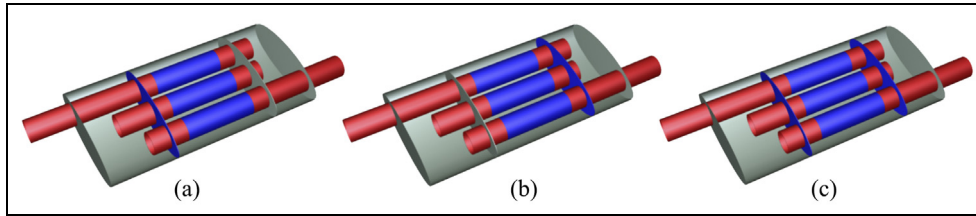
**Figure 13.** Geometry models of three-pass reactive muffler with perforated bulkheads: (a) perforated inlet bulkhead, (b) perforated outlet bulkhead, and (c) perforated inlet and outlet bulkheads (blue region: perforated portion; red region: solid portion).
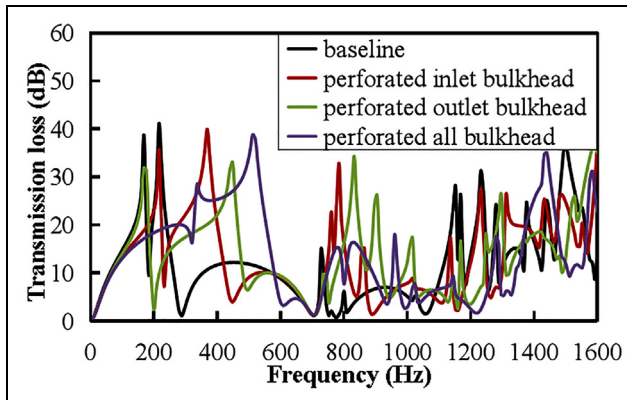


**Figure 14.** Effect of perforated bulkheads on transmission loss of three-pass reactive muffler (porosity $\phi = 6\%$ on bulkheads).
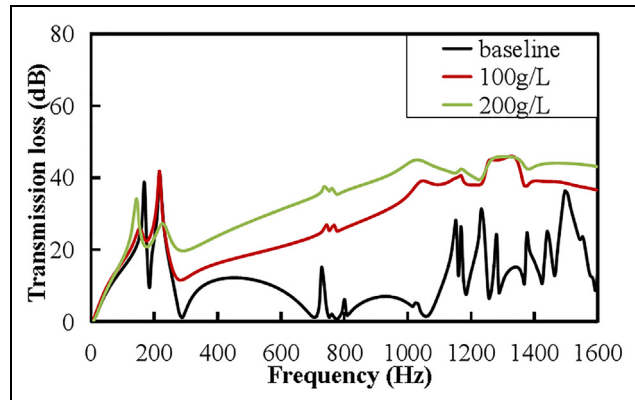


**Figure 16.** Effect of sound-absorbing material on transmission loss of three-pass perforated tube muffler.
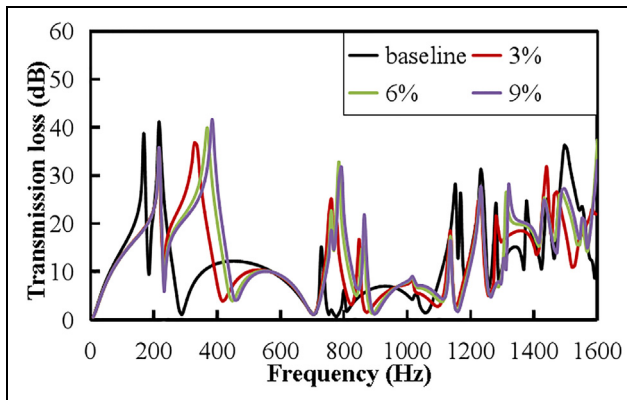


**Figure 15.** Effect of porosity of inlet bulkhead on transmission loss of three-pass reactive muffler.

Figure 18. The effect of perforation on the outlet tube within the middle chamber on the transmission loss is illustrated in Figure 19. It may be seen that decreasing number of holes improves the acoustic attenuation performance above 300 Hz in general. The influence of the perforation porosity of the outlet tube on the resonance peaks is not remarkable. Fixing the number of holes, the effect of bulk density of sound-absorbing material in the packed outlet tube is considered then. The higher

bulk density tends to improve the acoustic attenuation performance in the middle- to high-frequency range and barely affect the low-frequency acoustic attenuation as illustrated in Figure 20.

## Pressure drops

Figure 21 compares the pressure drop predictions from software ANSYS Fluent and measurements of the TPP muffler,[18] which validated the capability of Fluent for the pressure drop prediction of the TPP muffler. The software ANSYS Fluent is then employed to calculate the pressure drops for all configurations mentioned above.

The inlet BC in the computational fluid dynamics (CFD) simulation is set as the constant velocity 97.4 m/s. The outlet BC is set as the atmospheric pressure. The temperature of the fluid is 673 K. The sound-absorbing material is defined as porous region. At low Reynolds number, the pressure drop of sound-absorbing material is typically proportional to flow velocity. The coefficient between two variables equals the fluid viscosity divided by the permeability of porous material. An empirical correlation of permeability of fiberglass-like can be found from the work by Jackson and James[19]
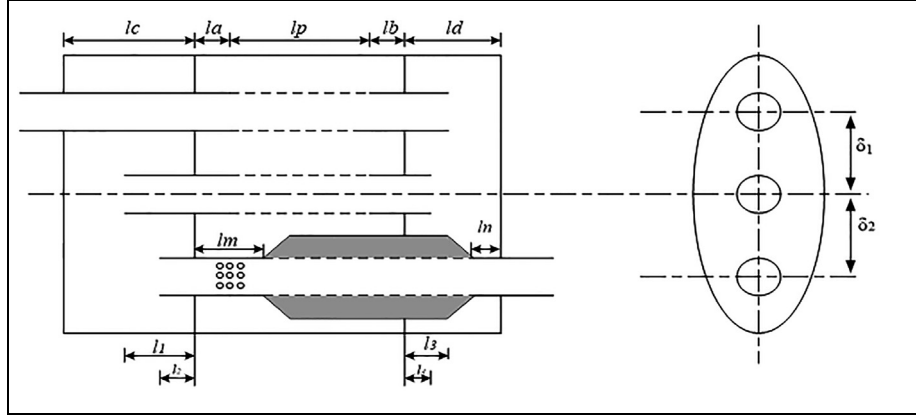
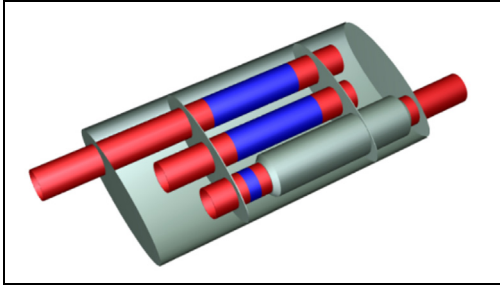**Figure 17.** Three-pass hybrid muffler with packed outlet tube.



**Figure 18.** Geometry of three-pass hybrid mufflers with packed outlet tube (blue region: perforated portion; red region: solid portion).
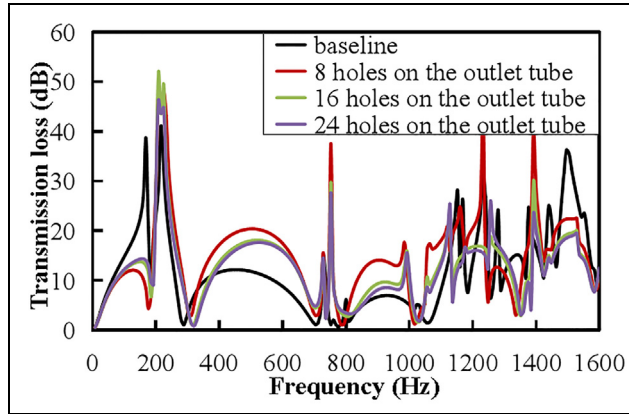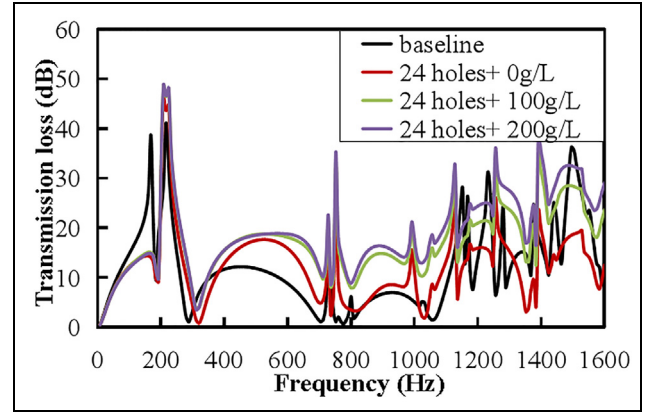


**Figure 20.** Effect of bulk density of sound-absorbing material in sleeve tube on transmission loss of three-pass hybrid muffler with packed outlet tube.
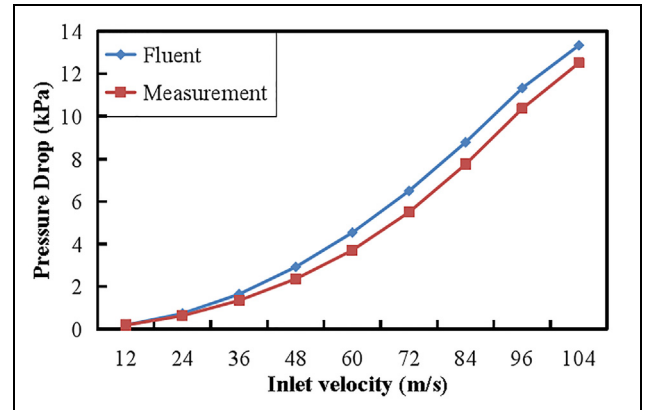


**Figure 19.** Effect of number of holes on outlet tube on transmission loss of the three-pass hybrid mufflers with packed outlet tube.



**Figure 21.** Fluent and experimental results of prototype TPP muffler.

$$\beta_f = \frac{d_f^2}{\left(64\varphi_f^{1.5}\left(1 + 56\varphi_f^3\right)\right)} \qquad (14)$$

where $d_f$ is the average diameter of the fiberglass and $\varphi_f$ is the porosity of the material.

Figure 22 compares the pressure drops of all muffler configurations. When the perforated inlet or outlet tube is replaced by the solid tube, the pressure drop is
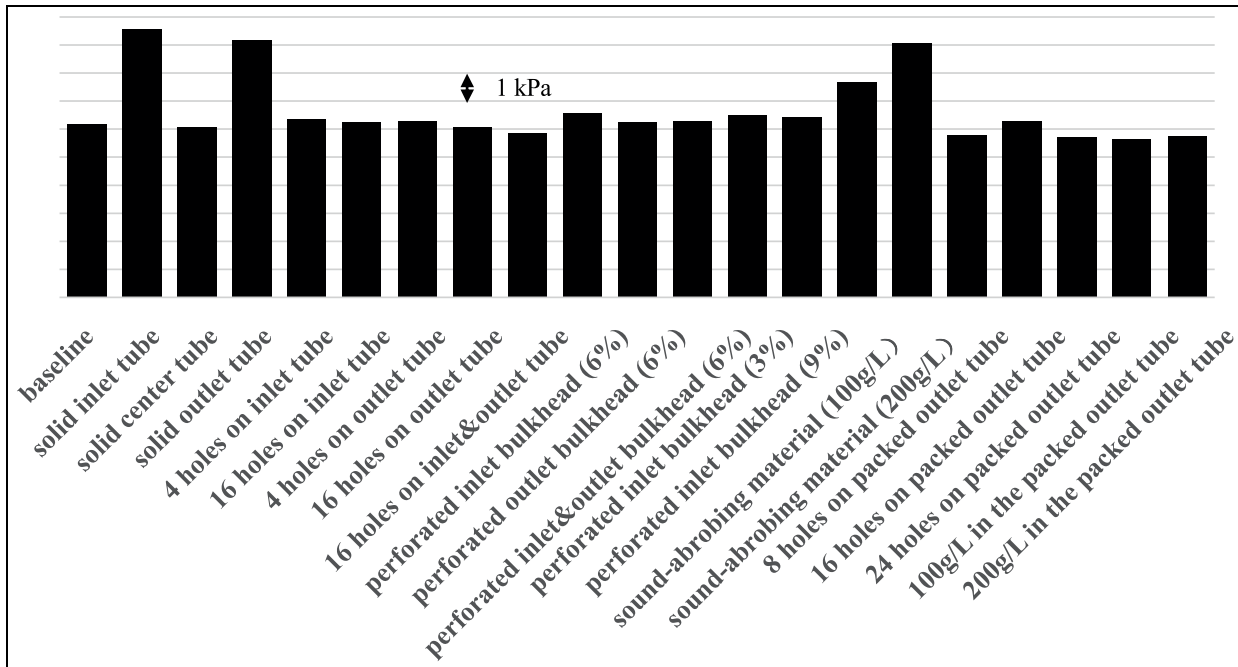
**Figure 22.** Comparison of the various pressure loss results of different configurations.

increased to about 1.5 times of the baseline value. Replacing the perforated center tube by the solid tube, the pressure drop keeps the almost same level as the baseline. The effect of perforation on the inlet or outlet tube within the end cavities on the pressure drop is not remarkable. When both the inlet and outlet tubes are perforated within the end cavities, the pressure drop is reduced slightly. As increasing porosity of perforated bulkhead, the pressure drop cannot be changed synchronously. It may be seen that the pressure drop of the muffler increases as increasing the bulk density of sound-absorbing material. The configurations of the hybrid muffler with packed outlet tube reduce the pressure drop to the baseline, except for the configuration with 16 holes on packed outlet tube.

## Conclusion

The FEM is employed to predict the transmission loss of TPP mufflers. The rigid inlet or outlet tube within the center chamber is found to remove the corresponding end resonator while enhancing the acoustic attenuation in the mid-frequency range. Replacing the perforated center tube by the solid one shifts the resonance to lower frequency. Increasing number of holes on the inlet/outlet tube(s) within the end cavities may affect the resonance(s). Decreasing the porosity of the perforated bulkhead shifts the resonance to lower frequency.

The higher bulk density of sound-absorbing material may improve the acoustic attenuation performance of the TPP tube hybrid muffler at mid–high frequencies

and shift the first resonance to lower frequency somewhat. For the three-pass mufflers with packed outlet tube, decreasing the number of holes improves the acoustic attenuation performance above 300 Hz in general. Fixing number of holes, the higher bulk density leads to the better acoustic attenuation in the middle-to high-frequency range and barely affects the acoustic attenuation performance at low frequencies.

The software ANSYS Fluent is employed to calculate the pressure drops of the mufflers. The numerical results showed that (1) the rigid inlet or outlet tube within the center chamber is found to increase the pressure drop and (2) the pressure drop of the muffler increases as the bulk density of sound-absorbing material increases.

## Declaration of conflicting interests

The author(s) declared no potential conflicts of interest with respect to the research, authorship, and/or publication of this article.

## ORCID iD

Hongpu Huang https://orcid.org/0000-0003-1322-2270

## References

1. Dickey NS, Selamet A and Novak JM. Multi-pass perforated tube silencers: a computational approach. *J Sound Vib* 1998; 211: 435–448.
2. Munjal ML. Analysis of a flush-tube three-pass perforated element muffler by means of transfer matrices. *Int J Acoust Vib* 1999; 2: 63–68.
3. Munjal ML. Analysis of extended-tube three-pass perforated element muffler by means of transfer matrices. *Proceedings of the fifth international congress on sound and vibration*, Adelaide, SA, Australia, 15–18 December 1997, pp.1701–1704. International Institute of Acoustics and Vibration.
4. Selamet A, Easwaran V and Falkowki AG. Three-pass mufflers with uniform perforations. *J Acoust Soc Am* 1999; 105: 1548–1562.
5. Ross DF. A finite element analysis of perforated component acoustic systems. *J Sound Vib* 1981; 79: 133–143.
6. Ji ZL and Selamet A. Boundary element analysis of three-pass perforated duct mufflers. *Noise Control Eng J* 2000; 48: 151–156.
7. Ji ZL and Fang FZ. Three-pass perforated tube muffler with end-resonator. SAE technical paper 2011-01-1529, 2011.
8. Munjal ML and Krishna VV. Flow-acoustic performance of a three-pass double-reversal muffler. SAE technical paper 2013-26-0106, 2013.
9. Verma A and Munjal ML. Flow-acoustic analysis of the perforated-baffle three-chamber hybrid muffler configurations. *SAE Int J Passeng Cars: Mech Syst* 2015; 8: 370–381.
10. Munjal ML. *Acoustics of ducts and mufflers*. 2nd ed. Chichester: Wiley, 2014.
11. Ji ZL and Fang Z. On the acoustic impedance of perforates and its application to acoustic attenuation predictions for perforated tube silencers. In: *Inter-noise*, Osaka, Japan, 4–7 September 2011. Institute of Noise Control Engineering.
12. Ji ZL. Boundary element acoustic analysis of hybrid expansion chamber silencers with perforated facing. *Eng Anal Bound Elem* 2010; 34: 690–696.
13. Delany ME and Bazley EN. Acoustical properties of fibrous absorbent materials. *Appl Acoust* 1970; 3: 105–116.
14. Lee IJ and Selamet A. Acoustic impedance of perforations in contact with fibrous material. *J Acoust Soc Am* 2006; 119: 2785–2797.
15. Tao Z and Seybert AF. A review of current techniques for measuring muffler transmission loss. SAE technical paper 2003-01-1653, 2003.
16. Marburg S. Discretization requirements: how many elements per wavelength are necessary? In: Marburg S and Nolte B (eds) *Computational acoustics of noise propagation in fluids: finite and boundary element methods*. Berlin: Springer, 2008, pp.309–332.
17. Fang Z and Ji ZL. Finite element analysis of transversal modes and acoustic attenuation characteristics of perforated tube silencers. *Noise Control Eng J* 2012; 60: 340–349.
18. Selamet A, Denia FD and Besa AJ. Acoustic behavior of circular dual-chamber mufflers. *J Sound Vib* 2003; 265: 967–985.
19. Jackson GW and James DF. The permeability of fibrous porous media. *Can J Chem Eng* 1986; 64: 364–374.